

# **Supporting Information**

## **A Fast Method of High-Frequency Induction Cladding Copper Alloy on Inner-Wall of Cylinder Based on Simulation and Experimental Study**

**Longlong He \*, Yafei Wang, Ruiyu Pan, Tianze Xu, Jiani Gao, Zhouzhou Zhang, Jinghui Chu, Yue Wu \***  
**and Xuhui Zhang**

Shaanxi Key Laboratory of Mine Electromechanical Equipment Intelligent Detection and Control, Xi'an University of Science and Technology, Xi'an 710049, China; wyf20160423@163.com (Y.W.); pry17835972904@163.com (R.P.); x13835872797@163.com (T.X.); gjn20190326@163.com (J.G.); helonger@gmail.com (Z.Z.); chujh@xust.edu.cn (J.C.); zhangxh@xust.edu.cn (X.Z.)  
\* Correspondence: hell@xust.edu.cn (L.H.); wuyue1992@xust.edu.cn (Y.W.)

Table S1 Experimental equipment parameters

Device	Name	Parameter
High frequency induction melting equipment	Model	RDGP-150B
	Input power	150kW
	Maximum Oscillation power	150kW
	Oscillation range	50-200kHz
	Input voltage	Three-phase 380v
	Cooling water pressure	0.2MPa
	Cooling water flow	>10L/min
Industrial cooling water circulation system	Model	ST-3AC
	compressor power	2.43kW
	Power	0.55kW
	Refrigerant	0.75HP
	Supply Voltage	R22
	Cooling method	380V/3 Ph/50Hz
	Refrigeration capacity	Air-cooled
Temperature detection equipment	Model	8.36kW
	Model	DTM-T1
	Measuring range	-50~1350 °C
	Measure the object distance ratio	20:1
	Accuracy	± 5 °C
	Emissivity	0.1~1.0
	Ambient Temperature	0 °C~40 °C

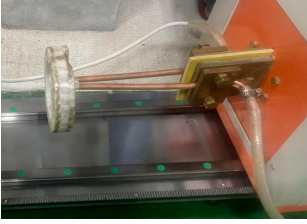
Workpiece rotation and translation device	Clamping and positioning	small three-jaw chuck
	Feed rate	2.0mm/s~2.5mm/s
	Cylinder rotation speed	40rad/s
Induction heating coil with magnetic conductor	Outer diameter of the magnetic core	116mm
	Inner diameter of the magnetic core	66mm
	Thickness of the magnetic core	25mm
	Application scope	20kHz~2000kHz
	Magnetic flux density	3700~4000MT
	Magnetic material density	4.8~5.2g/cm <sup>3</sup>

Table S2 Chemical composition of copper alloy cladding and cylindrical steel substrate

<b>Cladding</b>	<b>Element</b>	<b>Content /%</b>	<b>Matrix</b>	<b>Element</b>	<b>Content /%</b>
Copper-base alloy	Sn	18.050	Cylinder body	C	0.24-0.32
	Ni	18.260		Si	1.10-1.40
	Mn	0.823		Mn	1.10-1.40
	Al	≤0.002		P	≤0.035
	Fe	1.726		S	≤0.035
	Si	≤0.001		Cu	≤0.300
	Sb	≤0.001		Cr	≤0.300
	Bi	≤0.001		Mo	≤0.150
	Cu	Margin		Fe	Margin

Table S3 The microhardness value of the bonding interface

<b>Microhardness/HV</b>	-0.5	-0.4	-0.3	-0.2	-0.1	0	0.1	0.2	0.3
<b>Interface distance /mm</b>	Sample1	354.26	365.33	360.02	395.62	405.01	565.82	720.03	744.03
	Sample2	360.25	350.13	348.27	405.32	412.60	570.23	725.36	700.15
	Sample3	340.25	323.32	360.25	375.20	413.26	600.35	730.26	705.26
<b>Microhardness/HV</b>	0.4	0.5	0.6	0.7	0.8	0.9	1.0	1.1	1.2
<b>Interface distance /mm</b>	Sample1	743.63	746.65	630.25	450.65	226.35	238.45	228.67	232.54
	Sample2	745.87	650.25	745.45	755.26	745.46	460.25	223.46	228.98
	Sample3	740.30	700.35	750.30	755.20	745.25	480.36	230.25	226.35

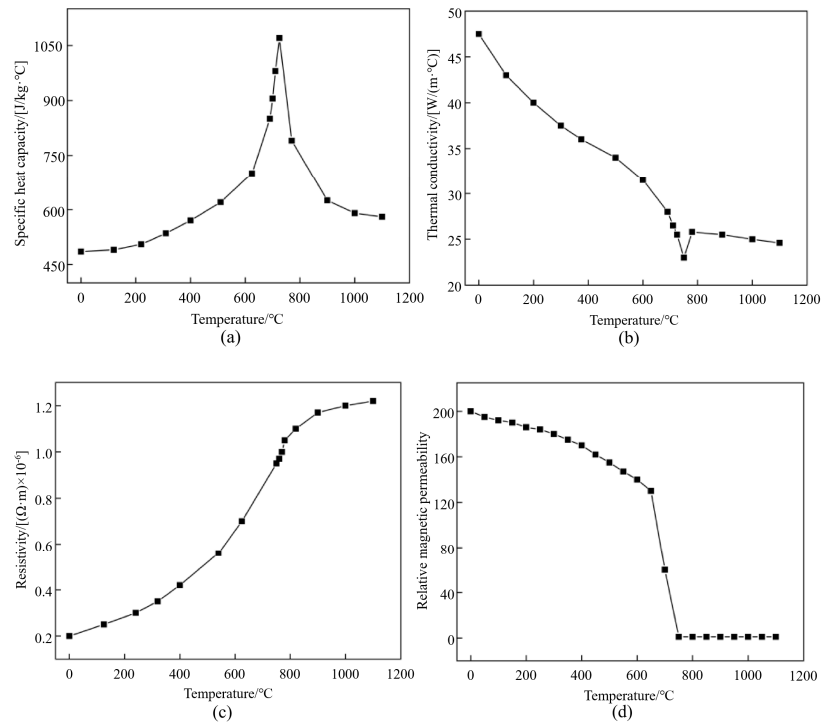


Figure S1. The physical parameters of the 27SiMn steel matrix change with temperature trends

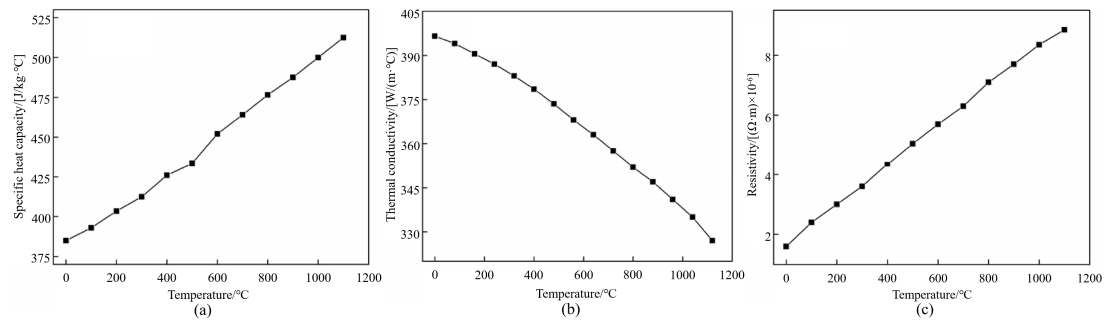


Figure S2. The physical parameters of copper alloys change with temperature trends

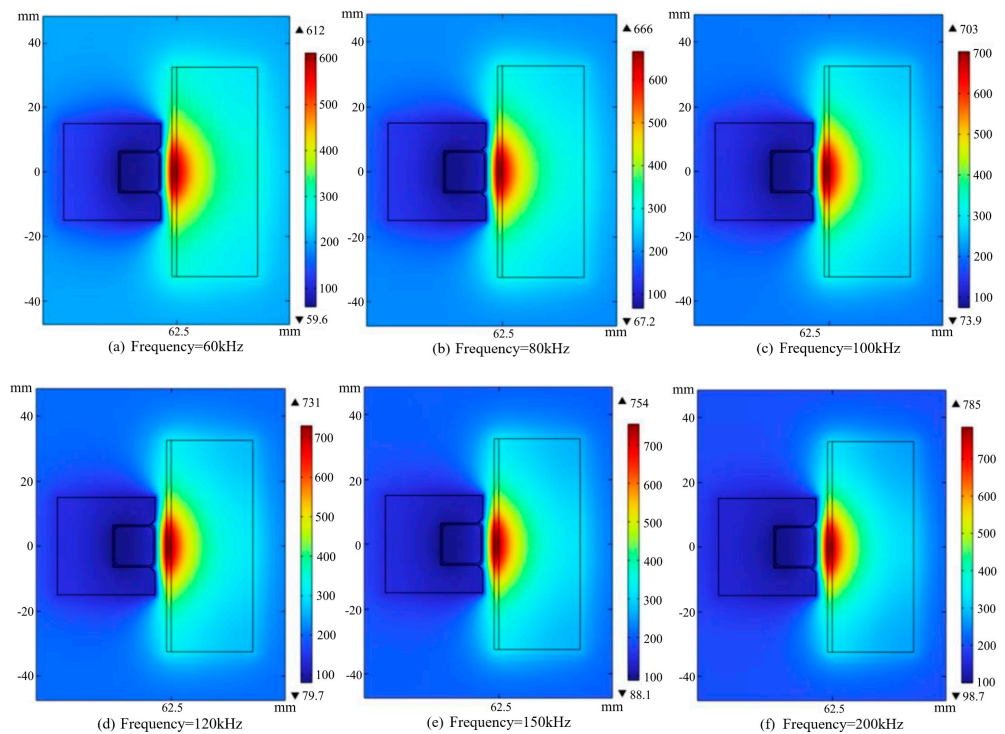


Figure S3. Temperature distribution at different frequencies at 3s

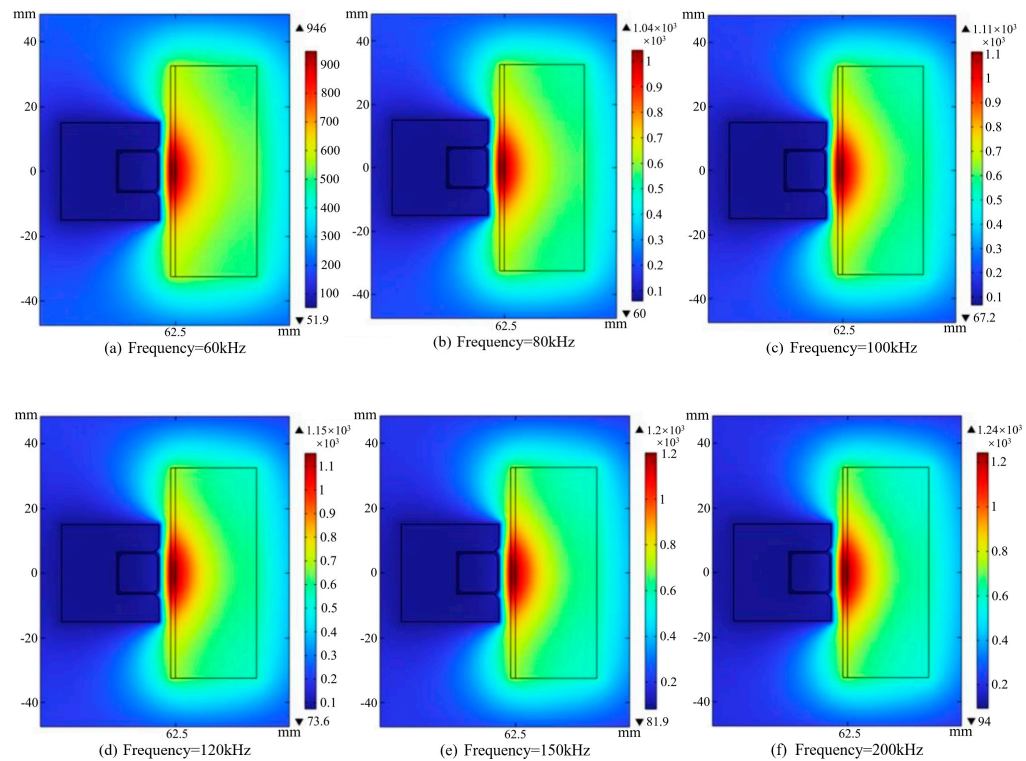


Figure S4. Temperature distribution at different frequencies at 9.5s

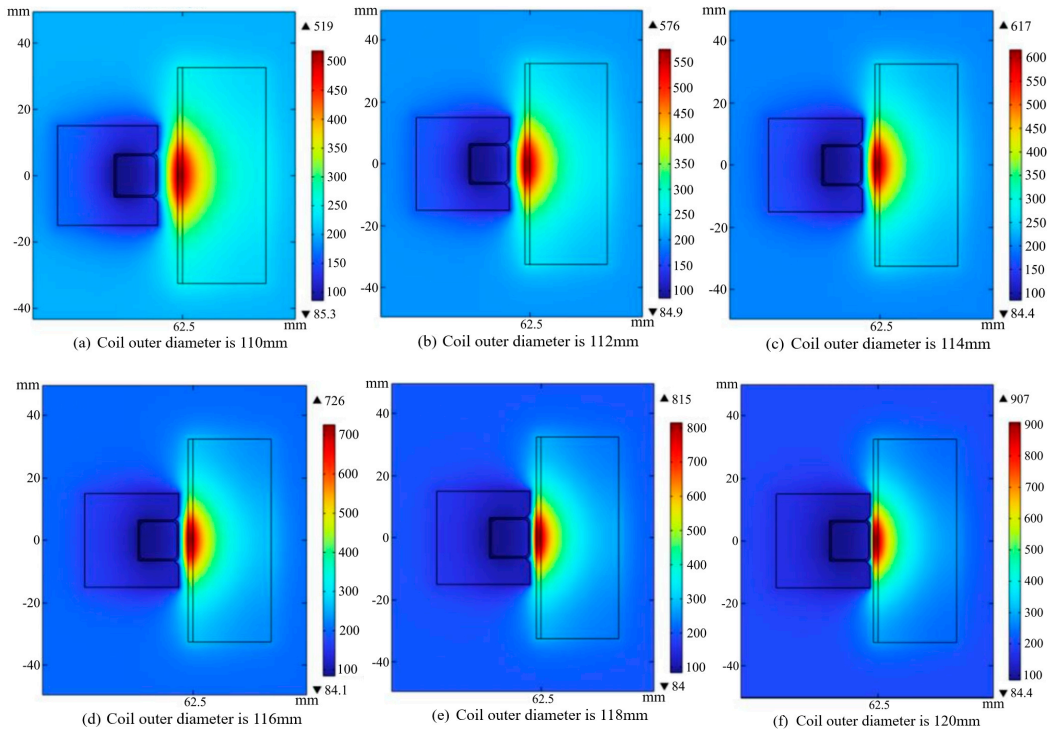


Figure S5. Temperature distribution under different outer diameters of induction coils at 2s

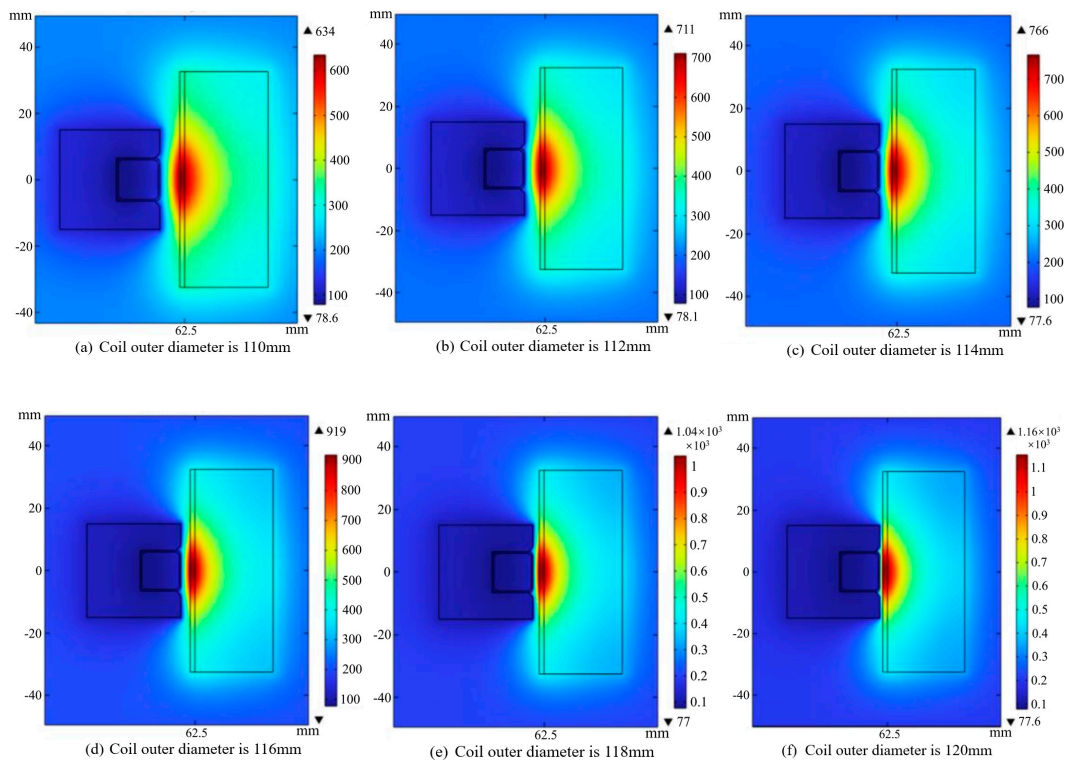


Figure S6. Temperature distribution under different outer diameters of induction coils at 4s

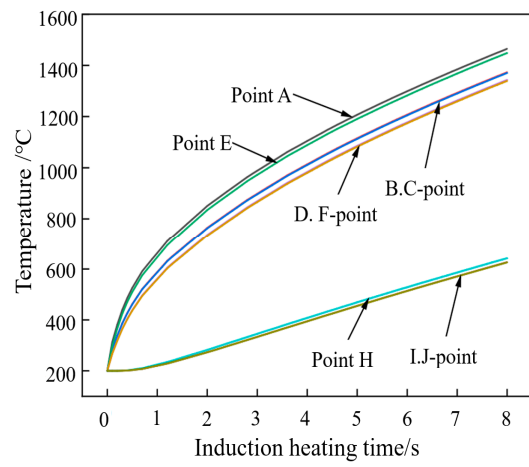


Figure S7. Simulate the thermal cycle curve of each point on a cylindrical workpiece

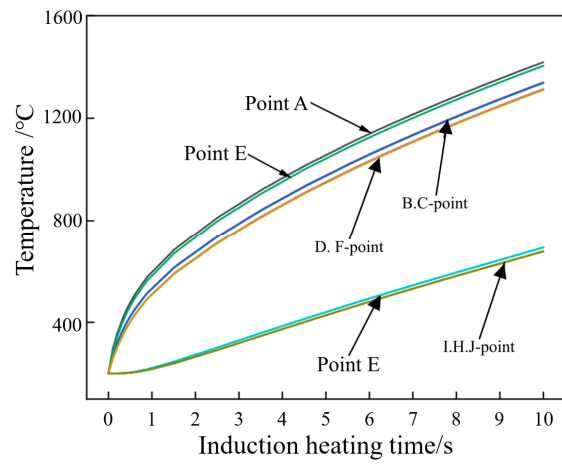


Figure S8. Simulate the thermal cycle curve of each point on the 2-cylindrical workpiece

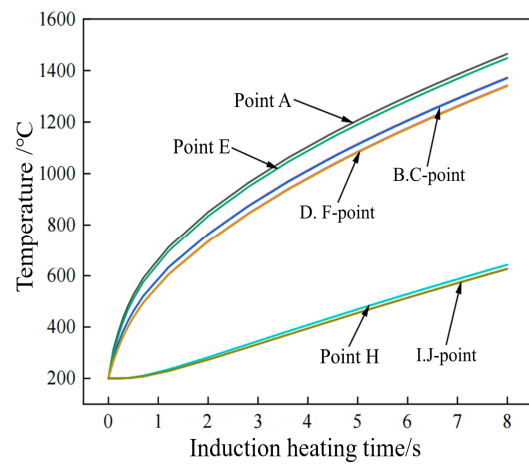


Figure S9. Simulate the thermal cycle curve of each point on the 3-cylindrical workpiece

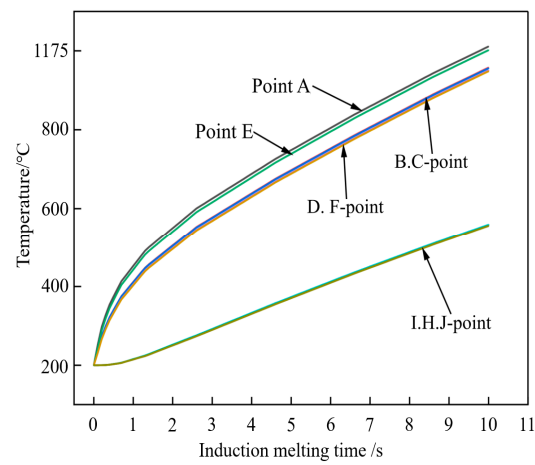


Figure S10. Simulate the thermal cycle curve of each point on the 4-cylindrical workpiece

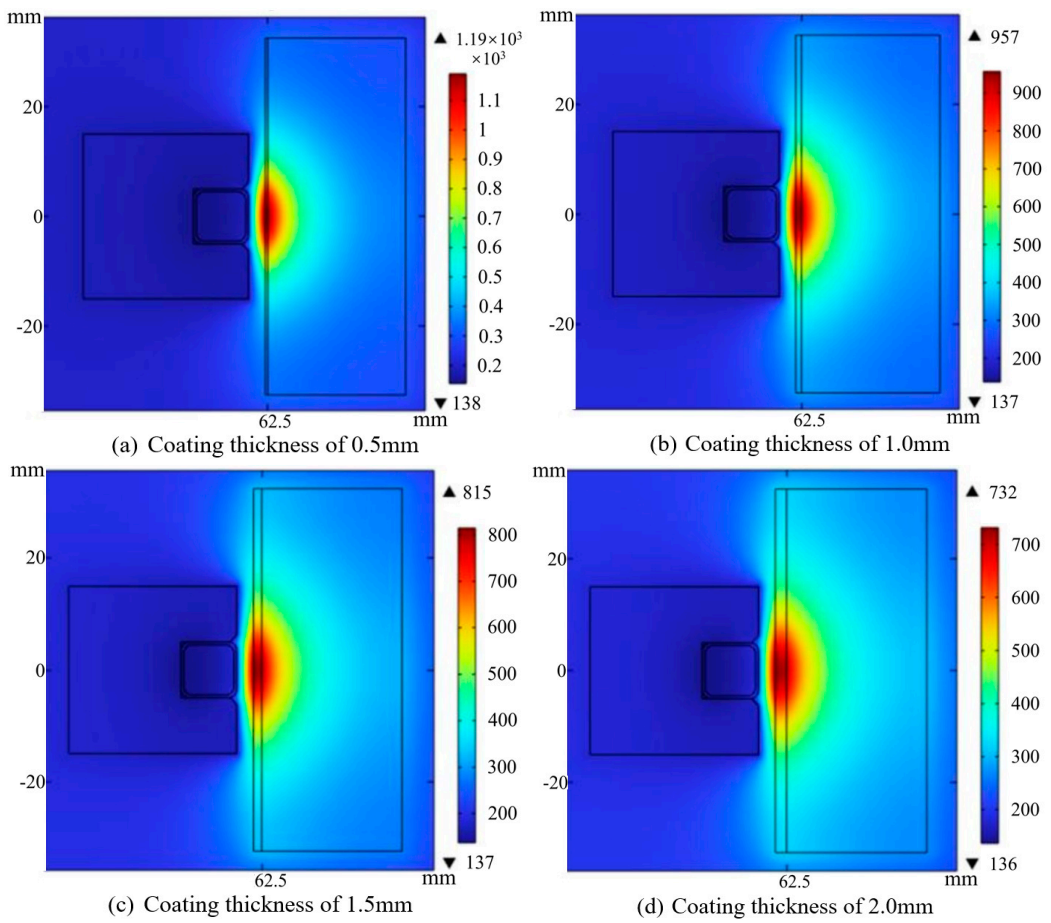


Figure S11. Temperature distribution of different cladding thicknesses at 3s

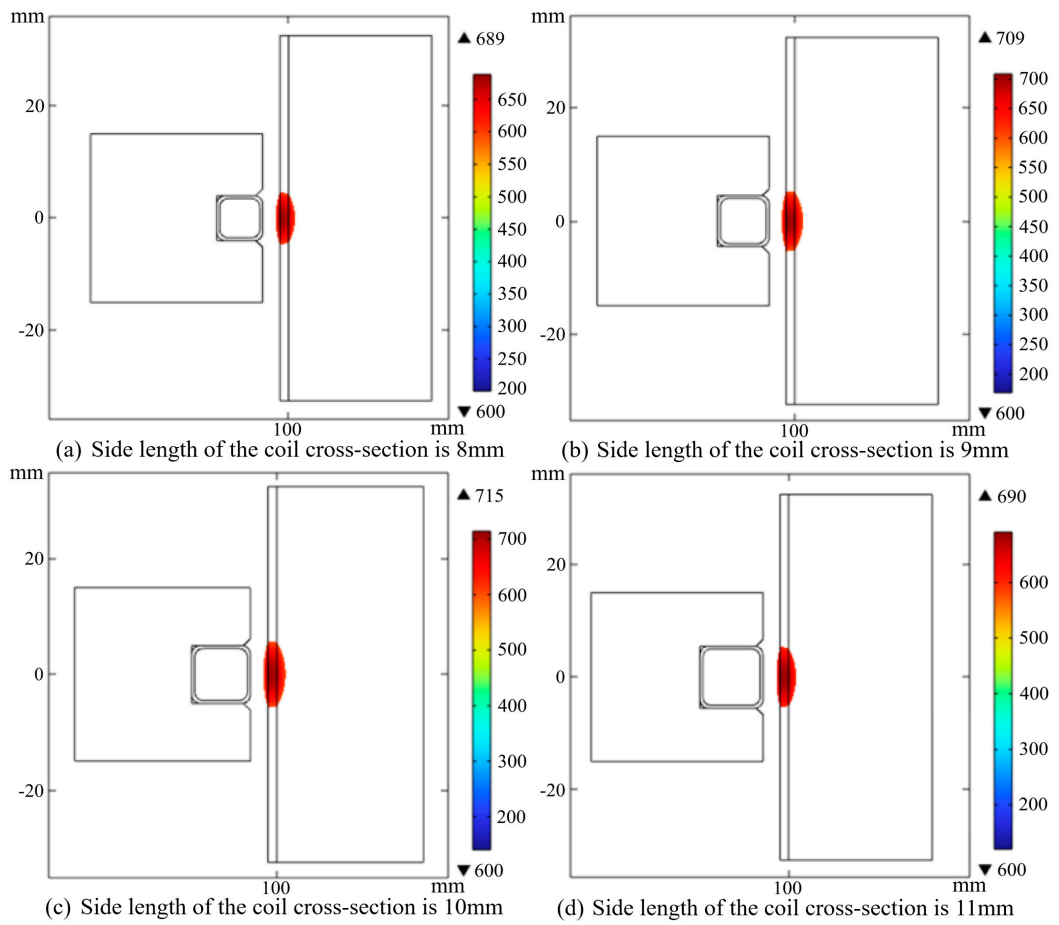


Figure S12. Temperature cloud map of the workpiece during 2s fusion of different cross-sectional edge lengths

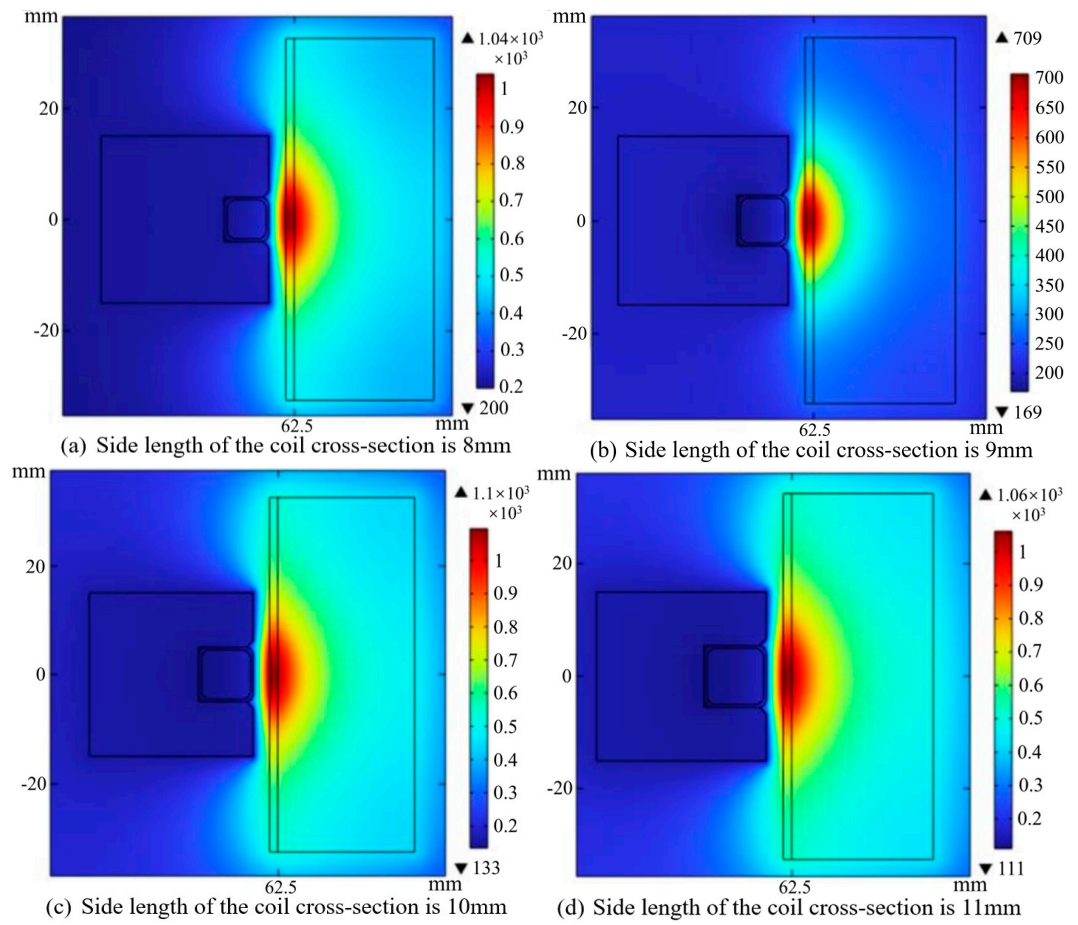


Figure S13. Temperature cloud map of the workpiece during induction melting for 6.5s



Figure S14. Schematic diagram of microhardness testing